MESH CONVERGENCE STUDIES FOR THIN SHELL ELEMENTS DEVELOPED BY THE ASME TASK GROUP ON COMPUTATIONAL MODELING

Gordon S. Bjorkman, Jr.
U.S. Nuclear Regulatory Commission

David P. Molitoris
Westinghouse Electric Company

Doug Ammerman
Sandia National Laboratories

Ginny Broz
Bettis Laboratory

Jeff Jordon
Savannah River National Lab.

Peter Shih
Transnuclear

Spencer Snow
Idaho National Laboratory

Chi-Fung Tso
ARUP, United Kingdom

Michael Yaksh
NAC International

Uwe Zencker
BAM, Germany

ABSTRACT

The ASME Task Group on Computational Modeling for Explicit Dynamics was founded in August 2008 for the purpose of creating a quantitative guidance document for the development of finite element models used to analyze energy-limited events using explicit dynamics software. This document will be referenced in the ASME Code Section III, Division 3 and the next revision of NRC Regulatory Guide 7.6 as a means by which the quality of a finite element model may be judged. One portion of the document will be devoted to a series of element convergence studies that can aid designers in establishing the mesh refinement requirements necessary to achieve accurate results for a variety of different elements types in regions of high plastic strain. These convergence studies will also aid reviewers in evaluating the quality of a finite element model and the apparent accuracy of its results.

In this paper the authors present the results of a convergence study for an impulsively loaded propped cantilever beam constructed of LS-DYNA thin shell elements using both reduced and full integration. Three loading levels are considered; the first maintains strains within the elastic range, the second induces moderate plastic strains, and the third produces large deformations and large plastic strains.

INTRODUCTION

Explicit finite element codes, such as LS-DYNA (Reference 1) and ABAQUS (Reference 2), used to analyze storage casks and transportation packages for energy-limited events, such as drop impact, puncture and aircraft crash, have evolved to become sufficiently sophisticated and robust as to be able

to predict the response to such events with reasonable accuracy. Such results are only achievable, however, by analysts who possess intimate knowledge of structural behavior and an understanding of how to properly construct a finite element model to produce accurate results using these codes.

In the hierarchy of finite element computational modeling complexity is explicit dynamic analysis, which is typically used to solve crash and impact problems, followed by implicit dynamic analysis, which is typically used to solve problems in forced vibrations and ground motion, and finally static analysis. Engineers who first encounter explicit dynamics codes, and who may be well versed in static analysis and implicit dynamics, soon become aware of the new challenges presented by crash and impact problems using explicit dynamics codes. To help address these new challenges, the ASME Task Group on Computational Modeling for Explicit Dynamics was formed in August 2008. The purpose of the Task Group is to create a quantitative guidance document for the development of finite element models used to analyze energy-limited events using explicit dynamics codes. This document will become a Non-Mandatory Appendix in the ASME Code Section III, Division 3 (Reference 3) and be referenced in the next revision of NRC Regulatory Guide 7.6 (Reference 4) as a means by which the quality of a finite element model may be judged.

Of all the considerations that go into constructing an accurate finite element model, the choice of element type and level of refinement of the element mesh are the most fundamental. Therefore, the Task Group's first undertaking was to develop a series of element convergence studies that can aid designers in establishing the mesh refinement requirements necessary to achieve accurate results for a variety of different elements types in regions of high plastic strain. Several mesh convergence studies have been completed and others are scheduled for completion in the near future. These include:

1. A propped cantilever beam subjected to a uniform impulsive load. Elements to be studied include hexahedral, thin shell and thick shell using both full and reduced integration.
2. A flat plate impacting a puncture bar. The plate and bar will be constructed from hexahedral elements using both full and reduced integration.
3. A right circular thin shell canister with a thick top lid subjected to an end drop onto a rigid surface. The impact will induce buckling into the shell and significant strains at the discontinuity between the shell and bottom plate. The model will be constructed from hexahedral elements using both full and reduced integration.
4. A right circular cylinder composed of thin shell elements being impacted by a near rigid sphere.

In this paper the authors present the convergence study results for the propped cantilever beam constructed of thin shell elements.

PROPPED CANTILEVER CONVERGENCE STUDY

The propped cantilever beam is 20 inches long and has a 1-inch square cross section. The loading condition is a downward uniformly distributed load of magnitude W applied on the top surface of the beam (y = d) as shown in Figure 1. The load ramps from zero to W over an interval of $t_r = 0.02$ sec. and then remains constant. Note that the pressure load remains oriented vertically throughout the beam deflection. At the fixed end, the boundary conditions are $u_y = 0$ at the bottom left edge (i.e., at x = y = 0) and $u_x = 0$ for the entire left face. At the propped end, the boundary condition is $u_y = 0$ at the bottom

right edge (i.e., at x = L, y = 0). The beam is analysed as a plane-strain problem with only one element through the width (z), so $u_z = 0$ for all nodes.

For thin shell elements, the boundary condition at the fixed end is established by setting all nodal degrees of freedom to zero (i.e., $u_x = u_y = u_z = rot_x = rot_y = rot_z = 0$). The boundary condition at the propped end is established by setting nodal degrees of freedom $u_y = u_z = rot_x = rot_y = 0$. Along the length of the beam, the plane-strain boundary condition is established by setting nodal degrees of freedom $u_z = rot_x = rot_y = 0$.

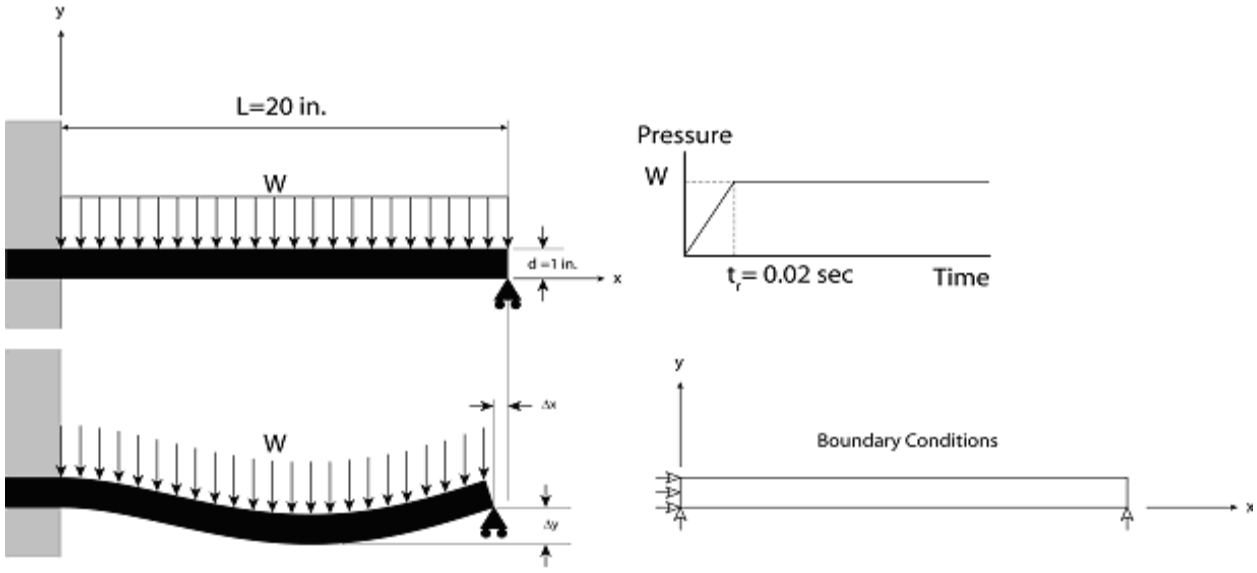

Figure 1: Propped Cantilever Convergence Study Problem.

The beam is made of Type 304 stainless steel with a yield strength of 30 ksi and an allowable stress intensity (S_m) of 20 ksi. The material model is a power-law hardening model: $\sigma = \sigma_y + A\varepsilon^n$, with σ_y = 30 ksi, strength coefficient A = 192 ksi, and hardening exponent n = 0.74819. The material has an elastic modulus E = 28e6 psi, a poisson's ratio $\nu = 0.3$, and a mass density of ρ = 7.39e-4 lbm/in^3.

Three pressure load cases are considered, 100 psi, 240 psi, and 500 psi. The smallest load case produces an elastic response while the other two loads produce different levels of plasticity. The two smaller loads are based upon the elastic design criteria of the ASME B&PV Code, Section III, Division 3, WB-3000, which gives an allowable membrane plus bending stress intensity of 1.5 S_m = 30 ksi for normal conditions of transport (NCT) and 3.6 S_m = 72 ksi for hypothetical accident conditions (HAC). The pressure loads required to produce these stresses were derived using elastic beam theory. For a propped cantilever beam under pressure loading the maximum bending moment occurs at the built-in end and is equal to $WL^2/8$. The stress associated with this moment is $\sigma = Mc/I = WL^2c/8I$. For this problem, L = 20 in., c = 0.5 in., and I = 1/12 in^4. For the NCT allowable stress limit of 30 ksi, the calculated load W is 100 lbs/in, which for a 1-inch wide beam equates to 100 psi. For the HAC allowable stress limit of 72 ksi, the corresponding load is 240 psi. The third load level of 500 psi is chosen to result in a much higher level of plasticity.

MODEL SETTINGS AND ASSUMPTIONS

The convergence study analyses are performed using LS-DYNA, Version: ls971d R4.2.1, Revision 53450, Double Precision. The material model used is *MAT_SIMPLIFIED_JOHNSON_COOK, which includes the power law relationship ($a + b\varepsilon^n$). The downward pressure load is applied using nodal force loading in order to maintain loading direction. Damping is applied well after full load application to damp out oscillations. Standard viscous hourglass control is used (Type 1, coefficient of 0.10), and all hourglass energy results were found to be acceptable. For the single point integration shell element, the Belytschko-Tsay shell element is used (Type 2) with stress and strain results reported at the outermost bottom and top integration points. For the full integration shell element, Type 16 is used with the 4 in-plane integration points averaged to the center of the shell. The averaged integration stress and strain results are reported at the outermost bottom and top integration planes.

CONVERGENCE STUDY RESULTS

Because the 500 psi loading case produced a wider variation in results than the 100 psi and 240 psi cases, and because the primary goal of the convergence study is to provide guidance for the development of accurate meshes in regions of high plastic strain, only the 500 psi load case results are reported. Also, it is important to note that the results for single point (reduced) integration and full integration were identical to within three significant figures, and therefore, only the single point integration results are reported.

Figure 2 is a plot of the maximum vertical displacement of the beam for various levels of mesh density (element length) for 2, 3, 5, 7 and 9 integration points through the shell thickness. The maximum displacement occurs at approximately x = 10.2 inches, and is the displacement after oscillations have been damped out. It is observed that displacement convergence is not uniform with increasing integration points as seen by the fact that 2 integration points underestimates the converged displacement while 3 integration points overestimates it.

Figure 3 is a plot of the convergence of the maximum bending stress at the top integration point of the beam at the cantilevered end, and occurs after all oscillations have been damped out. Figure 4 is a plot of the maximum effective plastic strain at the same location, which occurs before damping has been applied. In Figures 3 and 4, the results are reported at the center of the element closest to the cantilever (fixed) end. Because the center of the element where the integration point is located moves closer to the fixed end as the element length decreases, convergence is not achieved, as can be seen by the increasing slope of the curve as the elements become smaller.

To demonstrate a converged result requires that the integration point remain at the same location as the element length decreases. This condition is approximated in Figure 5, which is a plot of the maximum effective plastic strain at the location of maximum displacement. In this figure, it can be seen that the slope of the curve tends to zero as the elements become smaller.

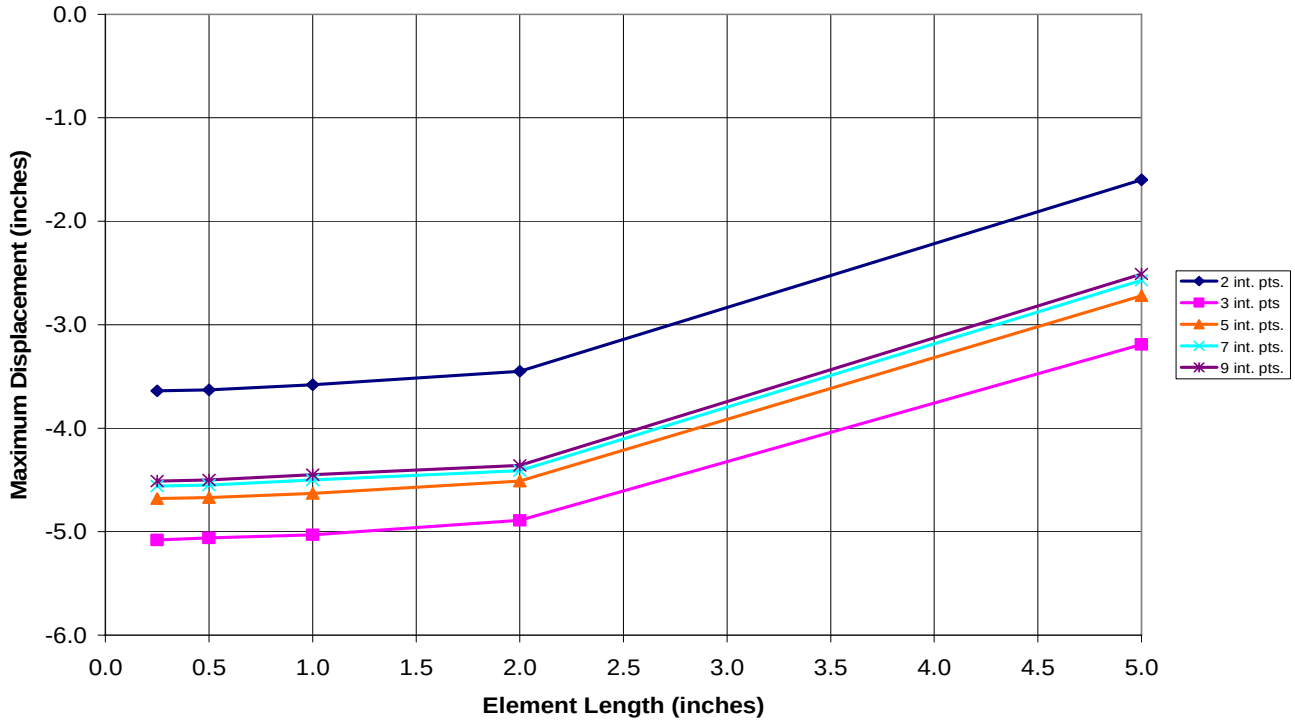

Figure 2: Maximum vertical displacement plotted against element length for various numbers of integration points through the thickness. (Single point integration thin shell, Type 2)

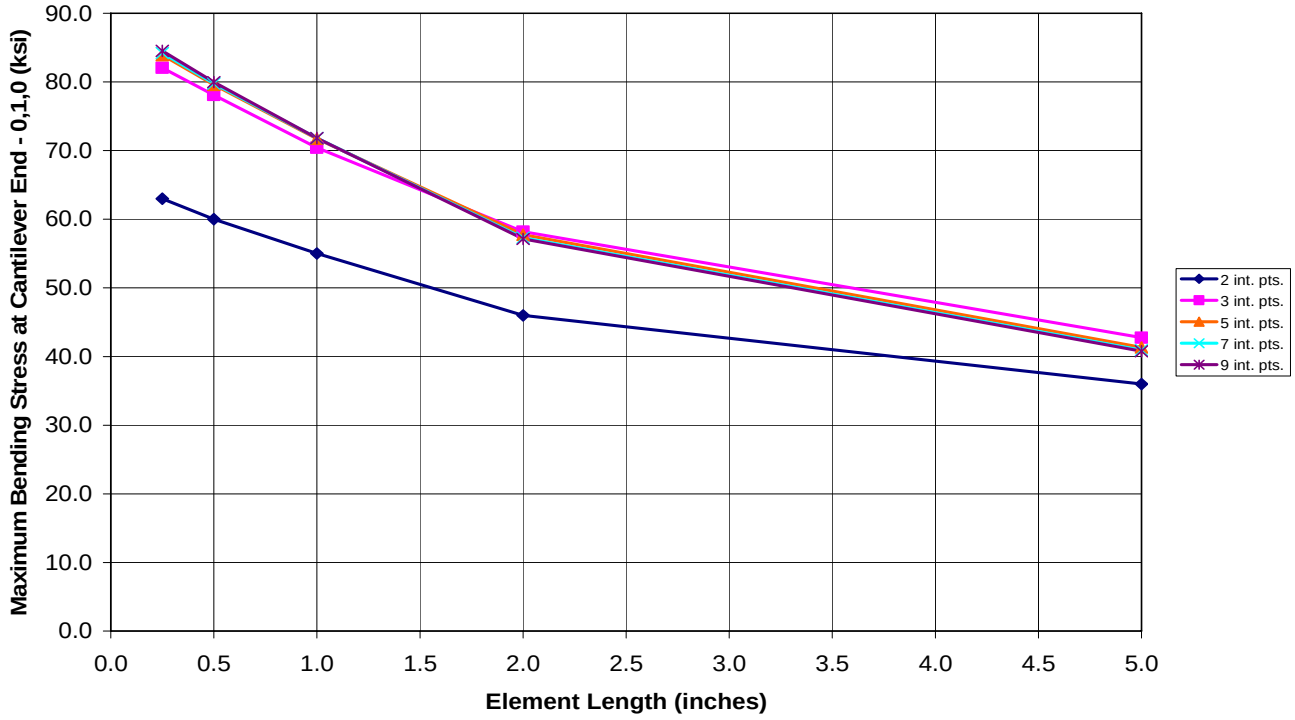

Figure 3: Maximum bending stress plotted against element length for various numbers of integration points through the thickness. (Single point integration thin shell, Type 2)

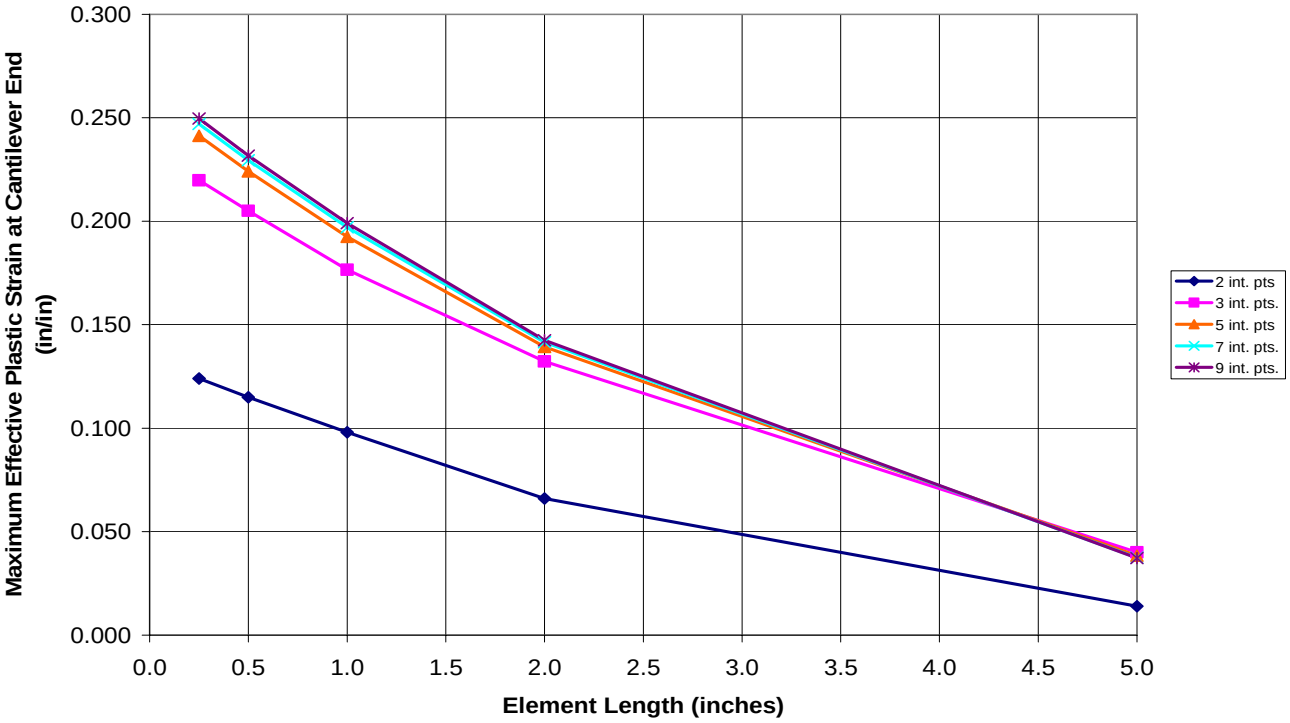

Figure 4: Effective plastic strain plotted against element length for various numbers of integration points through the thickness. (Single point integration thin shell, Type 2)

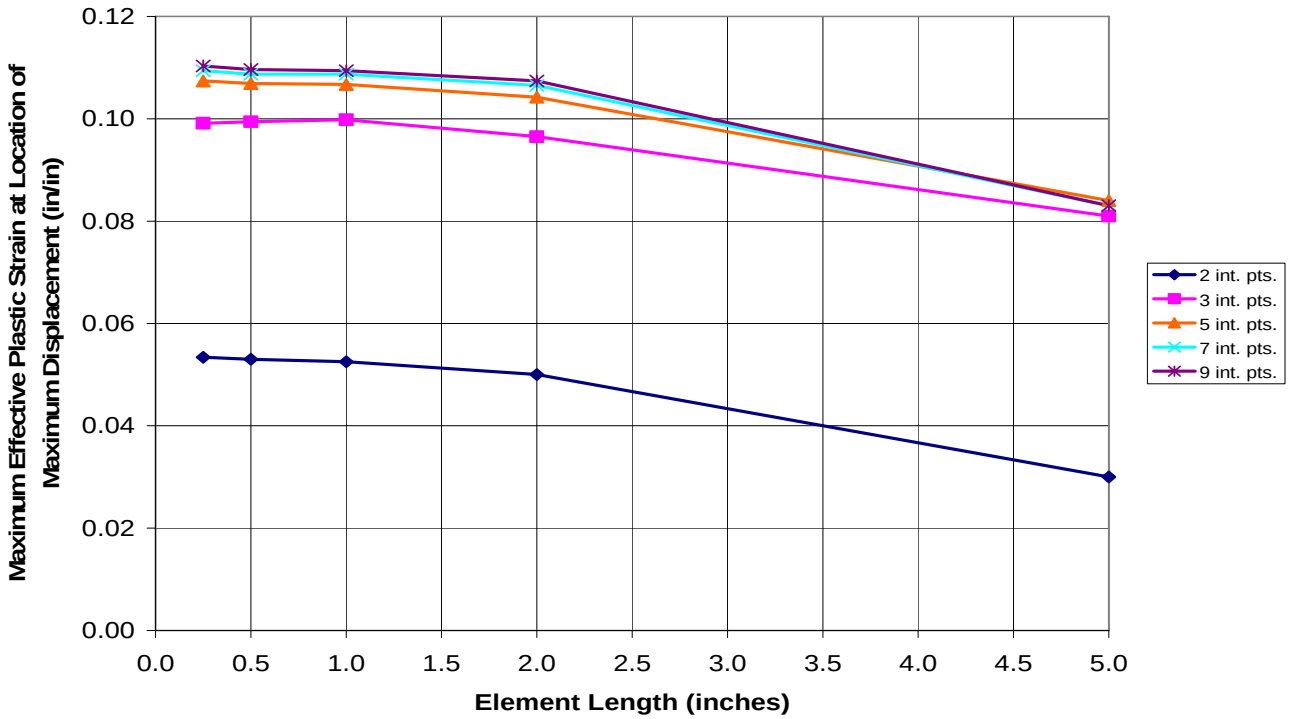

Figure 5: Maximum effective plastic strain at the location of maximum displacement plotted against element length for various numbers of integration points through the thickness. (Single point integration thin shell, Type 2)

It is recognized that thin shell element theory has inherent simplifications that could affect the accuracy of simulations under severe distortion (e.g., plane stress assumption). To gauge the accuracy of the thin shell results for this particular model and loading, it is instructive to compare the results to the same problem where the beam is meshed with hexahedral elements. For this comparison, a thin shell element with 9 integration points through the thickness is compared to the same beam problem meshed with 9 hexahedral elements through the thickness using single point (reduced) integration. Table 1 provides such a comparison for the top integration point in the element closest to the fixed end.

Table 1: Comparison of Thin Shell and Hexahedron Results

	Thin Shell	Hexahedron
Loading (psi)	500	500
No. Elements through Thickness	1	9
No. Integration Points per Element	9	1
Element Length (inches)	0.250	0.222
Max. Bending Stress(1) (ksi)	84.5	83.3
Max. Effective Plastic Strain(1) (in/in)	0.250	0.246
Max. Displacement	-4.51	-5.32

(1) Result is at the top integration point in the element closest to the fixed end.

It can be seen that the maximum bending stress and maximum effective plastic strain compare very well, but the maximum displacement results do not. The difference in maximum deformation can be attributed primarily to differences in the location of the applied load and boundary conditions and to a smaller extent, beam deformation modes that cannot be resolved by the thin shell elements. Specifically:

(1) The through thickness nodal boundary conditions at the fixed and propped ends are different for the thin shell and hexahedron meshes even though the global boundary conditions are the same.
(2) The thin shell element beam loads are applied at the mid-plane of the beam while in the hexahedron model the loads are applied at the top surface. It was found that this would effectively reduce the maximum displacement of the beam.
(3) The hexahedron mesh incurs high local deformation near the vertically supported bottom nodes.
(4) The thin shell elements cannot reproduce the shear deformation of the hexahedron elements particularly at the ends of the beam.

By comparison, for the 240 psi load case, where the maximum effective plastic strains were only on the order of 0.01 in/in, the maximum displacement of the thin shell beam and the hexahedron beam were identical.

CONCLUSIONS

From the results presented in Figures 2 through 5, it can be concluded that to achieve reasonable accuracy under bending requires at least 5 integration points through the thickness of a thin shell element, and that the maximum element length in regions of high strain gradients should be approximately equal to the thickness of the element. For problems involving large plastic strains, thin

shell elements can produce accurate stress and strain results within the limitations of thin shell theory (i.e., peak stresses at discontinuities cannot be captured), however, the assumptions inherent in thin shell theory may result in displacements being underestimated for severe loading conditions. In this particular model, the single point integration elements and fully integrated elements gave identical results, and there were no problems with element hourglassing. Therefore, for this application, there appears to be no computational advantage to using fully integrated thin shell elements.

REFERENCES

1. LS-DYNA, Livermore Software Technology Corporation, Livermore, CA.
2. Abaqus/Explicit, Dassault Systemes Simulia Corp., Providence, RI.
3. ASME Boiler & Pressure Vessel Code, Section III, Division 3, "Containments for Transportation and Storage of Spent Nuclear Fuel and High Level Radioactive Material and Waste," 2007.
4. Regulatory Guide 7.6, Revision 1, "Design Criteria for the Structural Analysis of Shipping Cask Containment Vessels," U.S. Nuclear Regulatory Commission, March 1978.